Supplementary Information

Selective and efficient detection of Pb^{2+} in aqueous solution by lanthanoids-organic frameworks bearing Pyridine-3, 4-dicarboxylic acid and glutaric acid

Zaib ul Nisa[a], Nargis Akhter Ashashi[a], Richa Singhaal[a], Musheer Ahmad[b], Rosa M. Gomila[c], Antonio Frontera[c],Haq Nawaz Sheikh[a,*]

[a]Department of Chemistry, University of Jammu, Baba Sahib Ambedkar Road, Jammu 180006, India

[b]Department of Applied Chemistry, Faculty of Engineering & Technology, Aligarh Muslim University, Aligarh, 202002, India

[c]Department of Chemistry, Universitat de les Illes Balears, Crts de Valldemossa km 7.5, 07122 Palma de Mallorca, Baleares, Spain

Table of Contents

CONTENTS **Page Number**

1. X-Ray Crystal structures of Ln-MOFs **1-5**

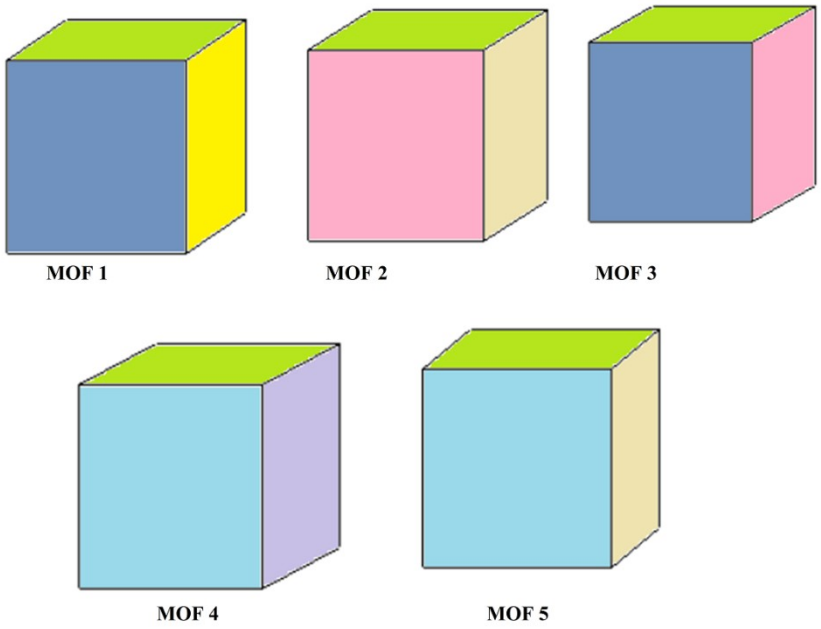

Figure S1. Shape of MOFs analyzed by Shape software

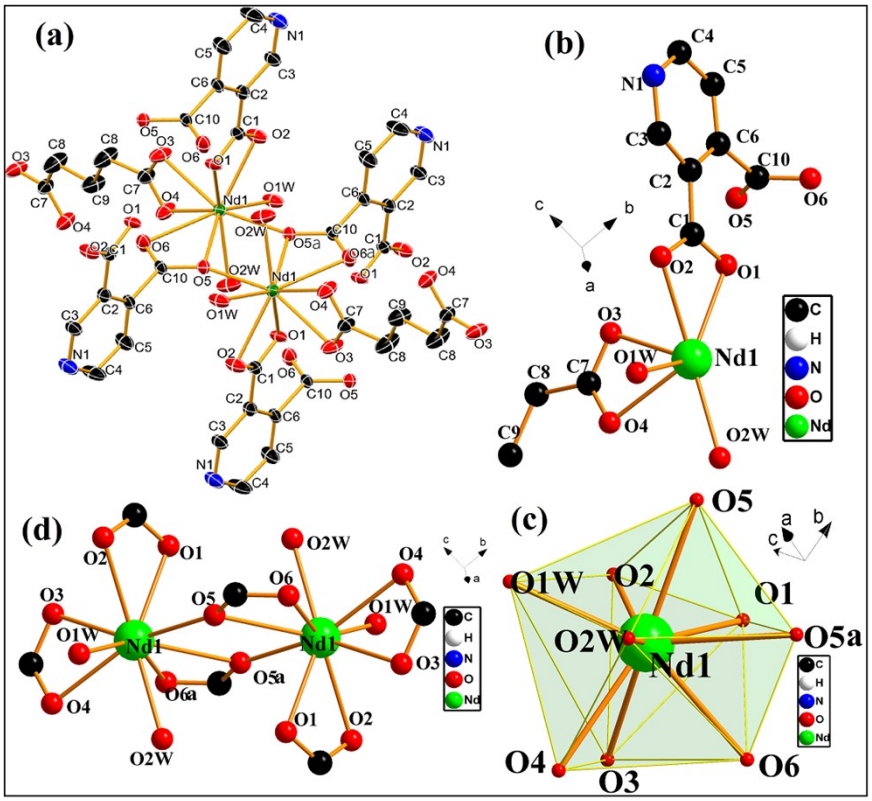

Fig. S2 Pictographic representation of the crystal structure of Ln-MOF **2**; (a) ORTEP view of the structural unit (the thermal displacement ellipsoids are drawn at 50% probability; H atoms are omitted for structural clarity); (b) Asymmetric unit of MOF **2** showing the coordination environment at the Nd site (guest solvent molecules are omitted for clarity); (c) MFF (muffin) polyhedral geometry around the Nd1 center (d) Representation of dinuclear Nd_2O_{16} SBU of Ln-MOF**2**

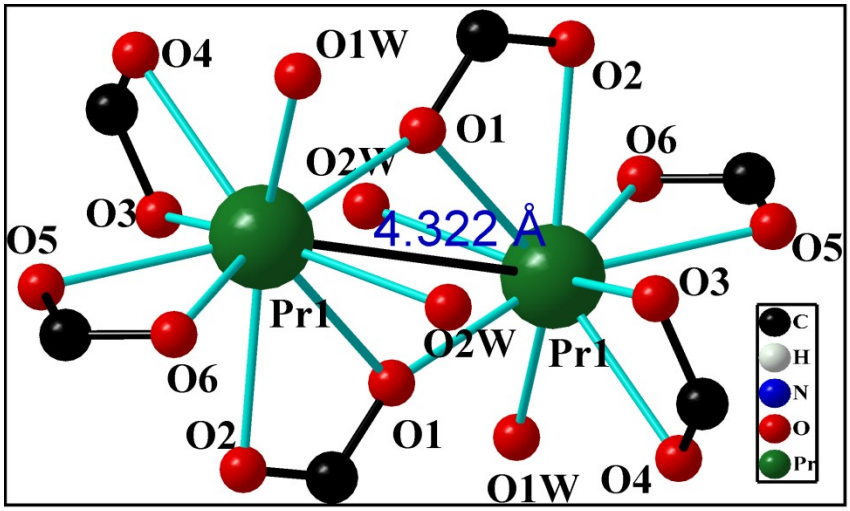

Figure S3. SBU of MOF **1**(Pr…Pr = 4.322 Å)

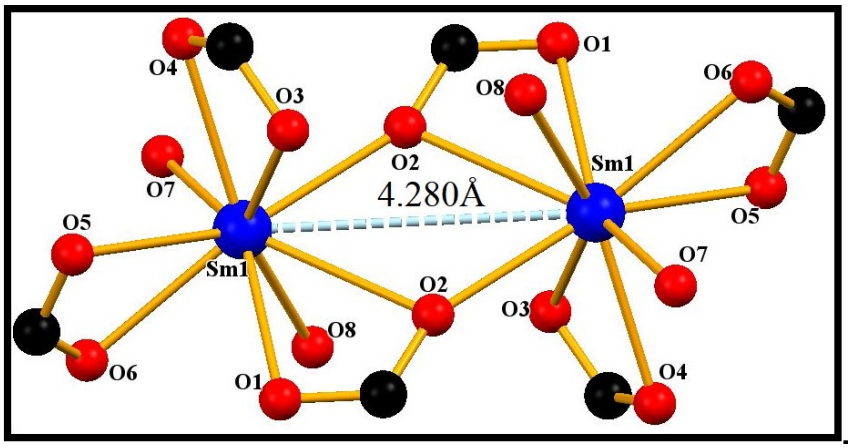

Figure S4. SBU of MOF **3**(Sm…Sm = 4.280 Å)

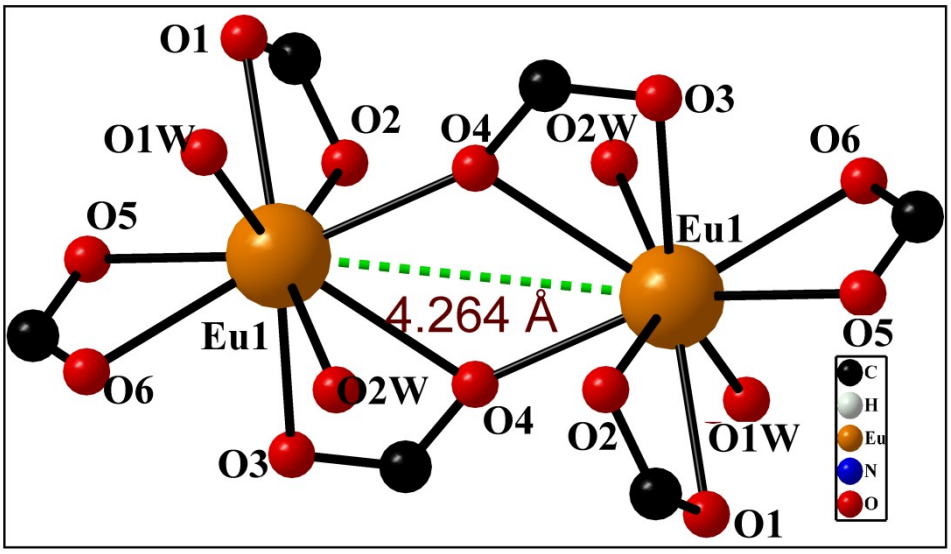

Figure S5. SBU of MOF **4**(Eu…Eu = 4.264 Å)

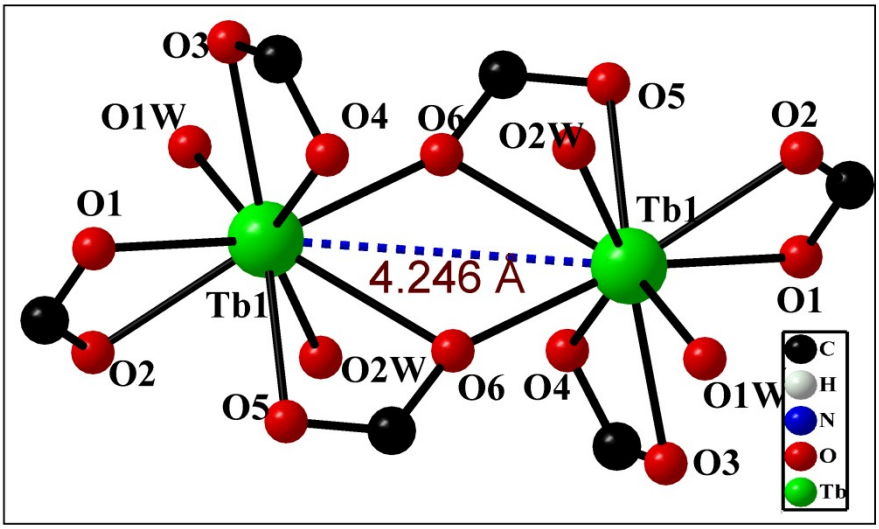

Figure S6. SBU of MOF **5**(Tb…Tb = 4.246 Å)

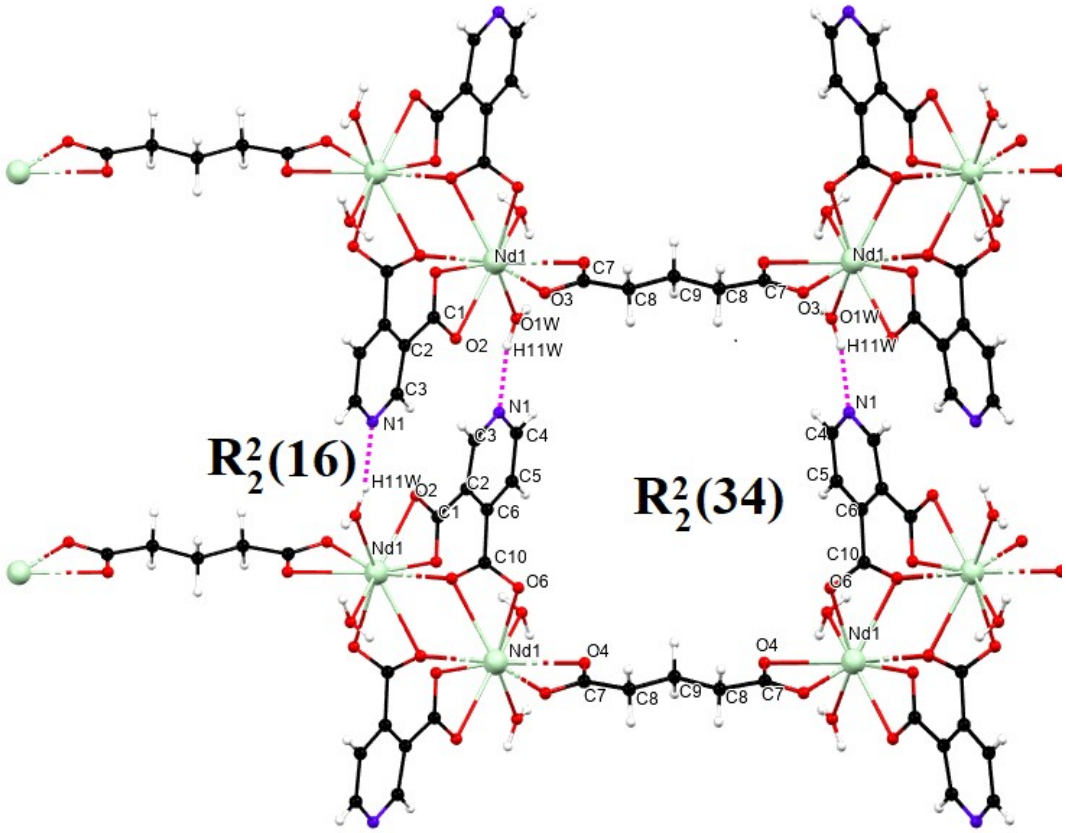

Figure S6. Presentation of the anionic portion of MOF **2** along the a-axis showing the R_2^2 (34) and R_2^2 (16) synthons.

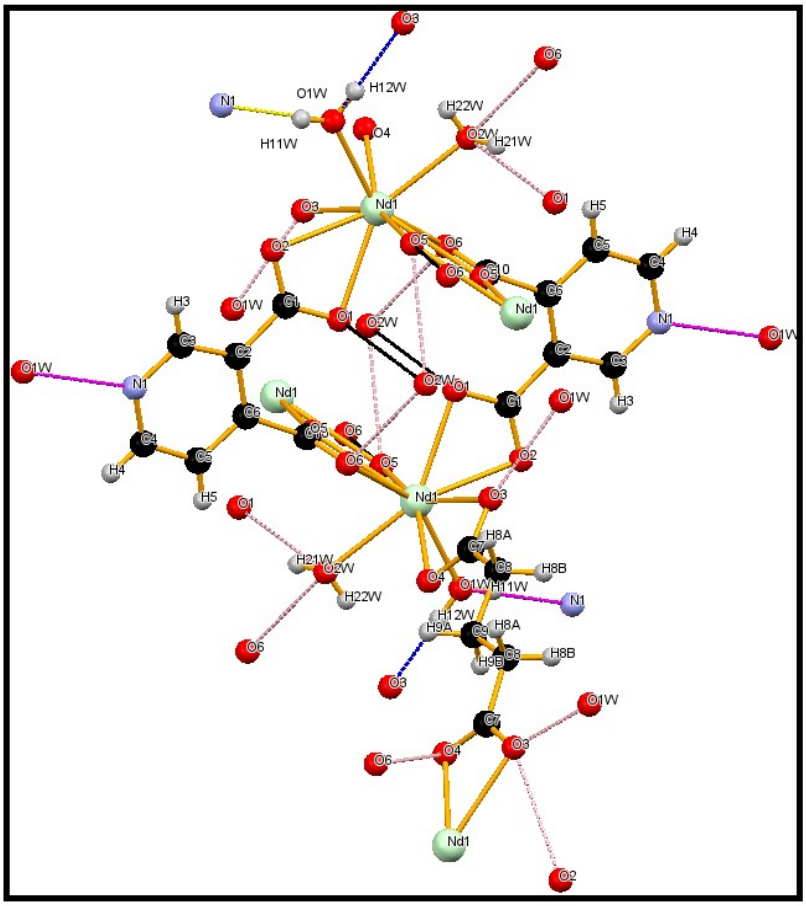

Figure S7. Hydrogen boding position of MOF**2**

2. Characterization by FTIR, PXRD, HSA, TGA

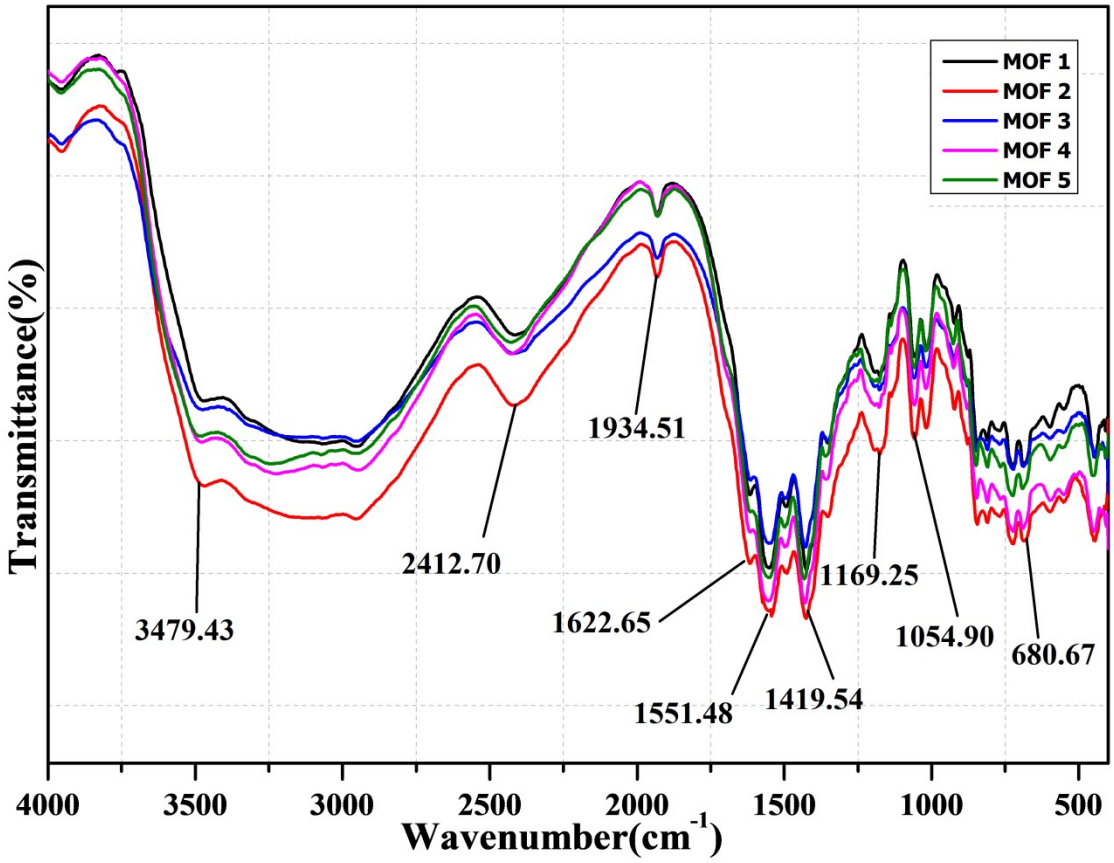

Figure S8. FTIR spectra of MOFs **1-5**

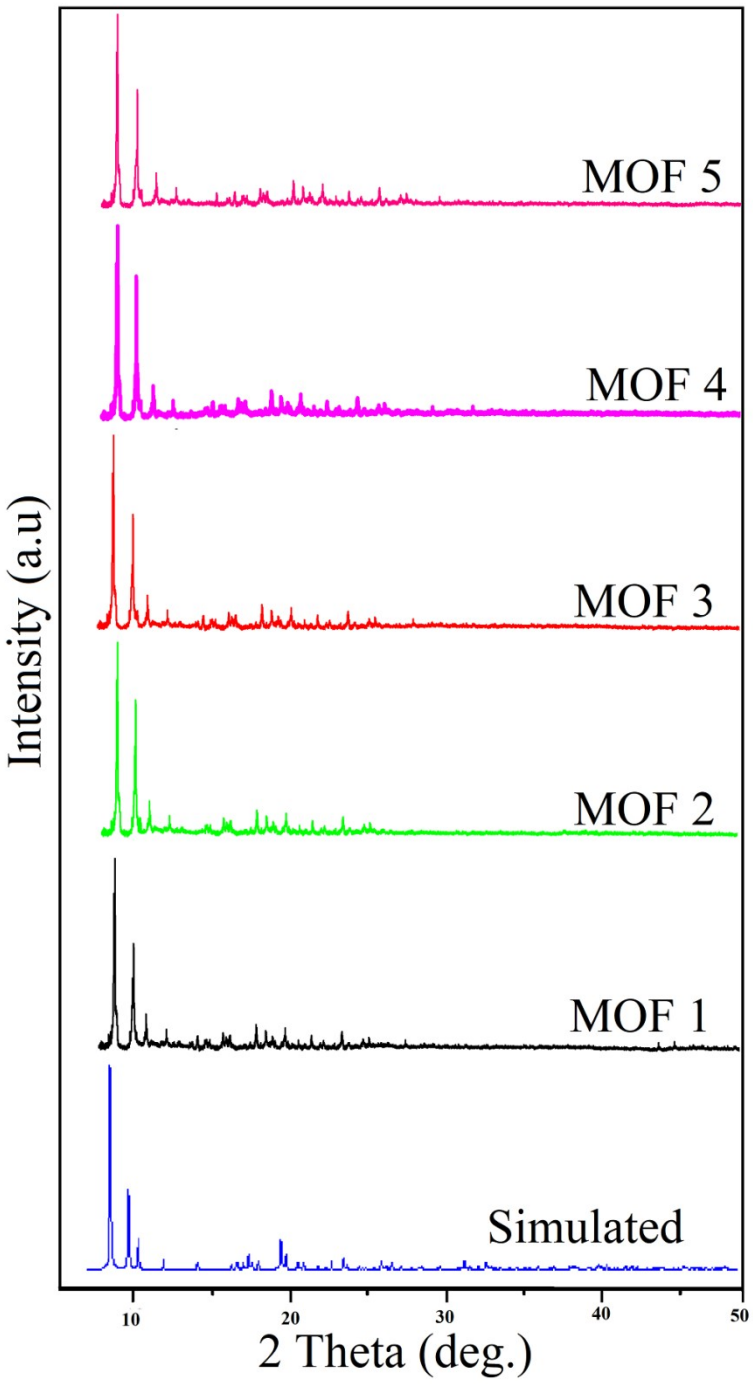

Figure S9. Experimental and simulated PXRD Patterns MOFs**1-5**

.

Thermogravimetric analysis

The obtained TGA curves, shown in Fig. S9-S10, suggest that complexes have typically four steps weight loss of as-prepared MOFs sample with increasing temperature. The first mass loss is about 5.62% (calculated 5.70%) below 135 °C, which can be attributed to the removal of one coordinated water molecule. The second weight loss between 135 and 325 °C is 5.67% (calculated 6.67%) resulting from the loss of second coordinated water molecule. With the increasing temperature, the mass loss of step three 3 is 25.63% from 325 C to 460 °C may be attributed to the loss of oxygen containing ligands and then decomposition of aromatic rings in fourth step. In addition, a temperature of 500 °C was found to be enough to remove all the organic frameworks and form metal oxides.[1-3]

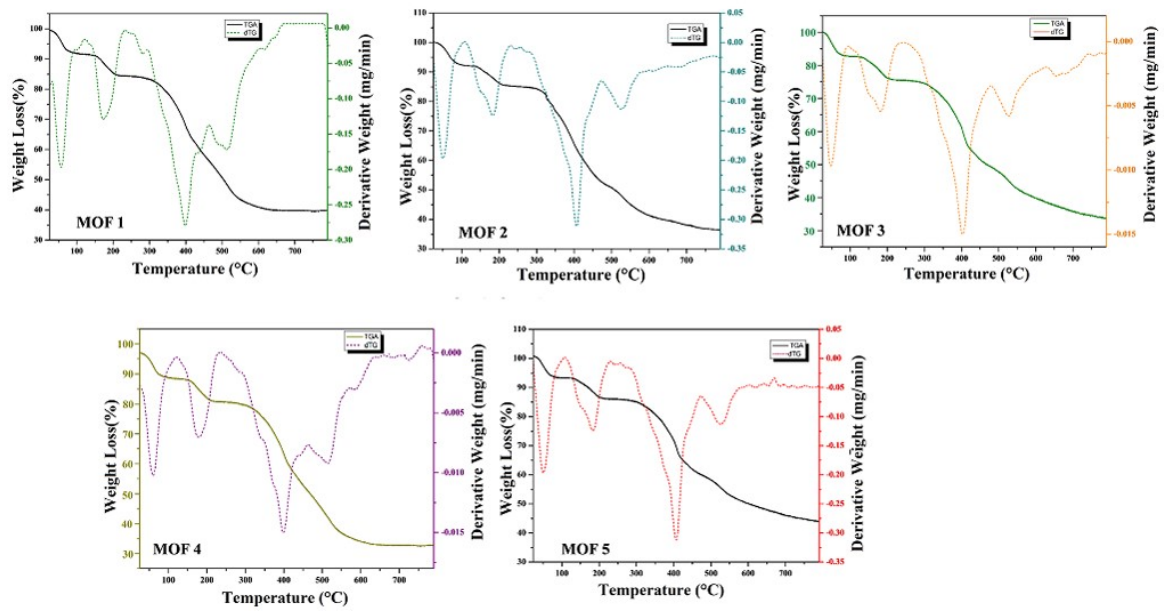

Figure S10. TGA curve and dTG curves for MOF **1**-MOF **5**

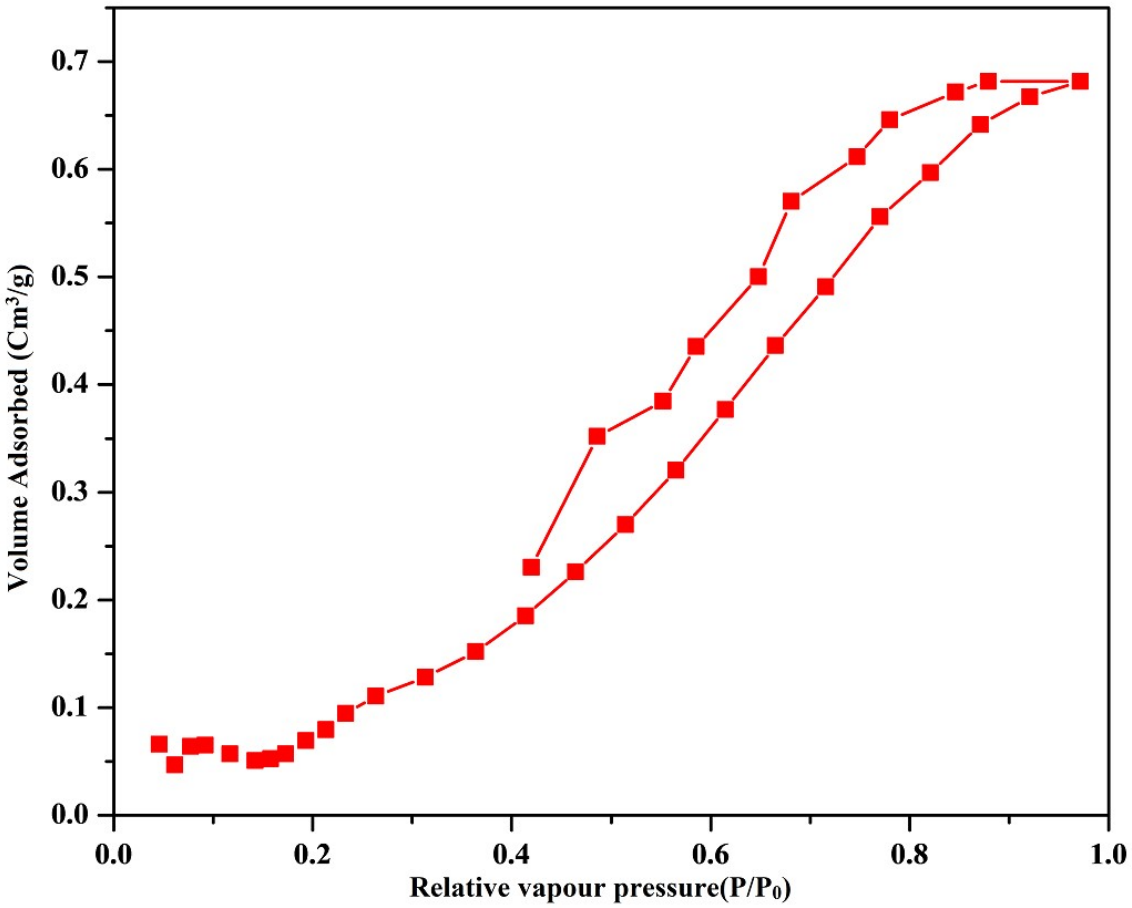

Figure S11. Nitrogen gas sorption isotherm at 77K for the activated Ln-MOF **2**

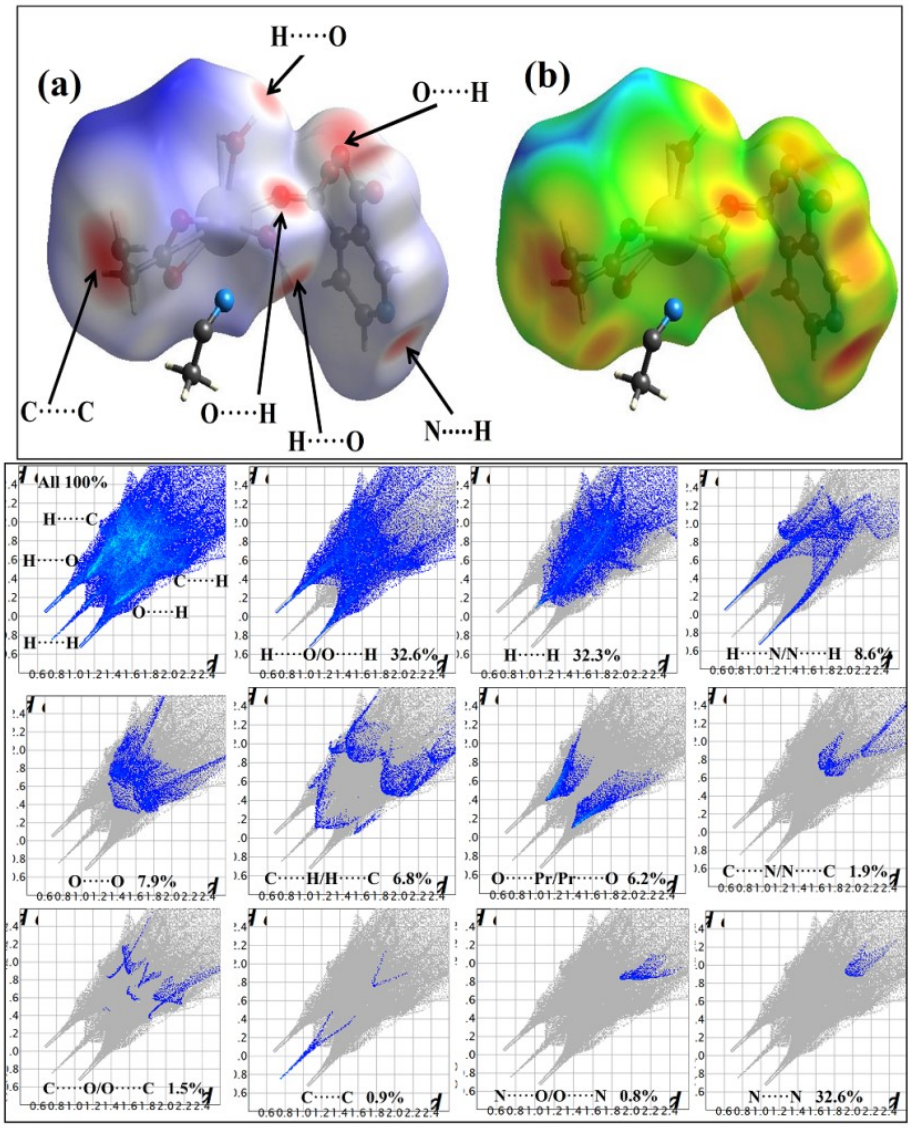

Figure S12. The semitransparent HSA drawn on fragments of MOF**1** (a) mapped with the d_{norm} (left)function (b) d_e (right). Regions of the most important intermolecularcontacts are indicated with arrows. Redovals indicate regions in which HS are ‘‘perforated’’ by coordinationbonds. Fingerprint plots ofMOF**1** showing the percentages of contacts to the total Hirshfeld surface area of molecules

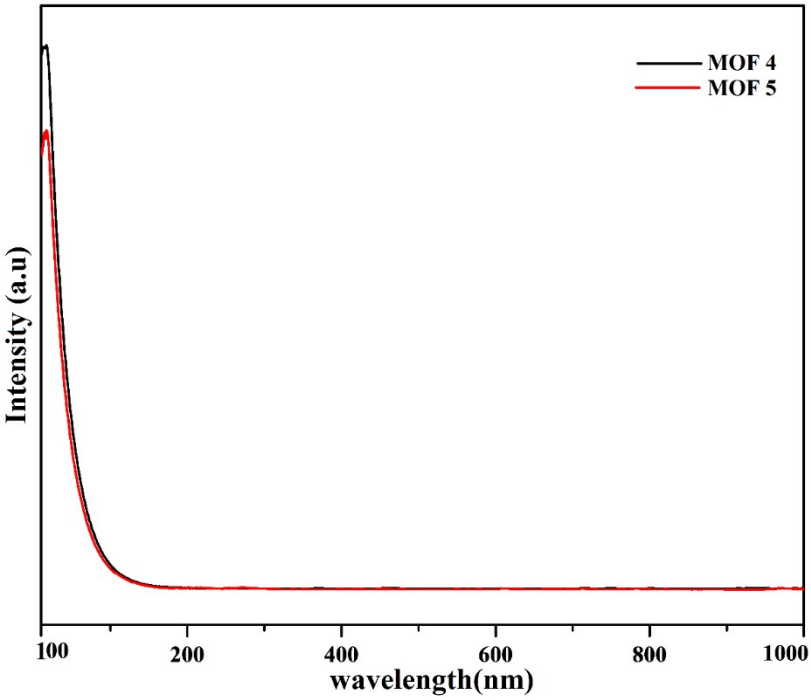

Figure S13. Lifetime curves of MOFs **4** and **5**

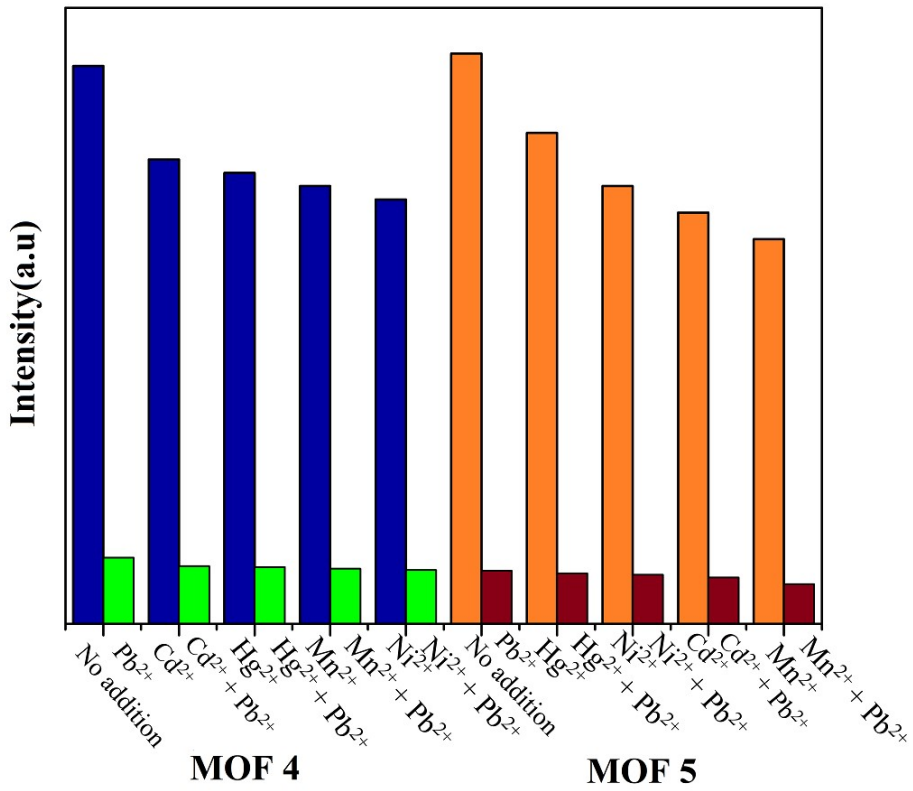

Figure S13. Selectivity experiment for Pb^{2+} in the presence of other metal ions for MOF 4 and MOF 5.

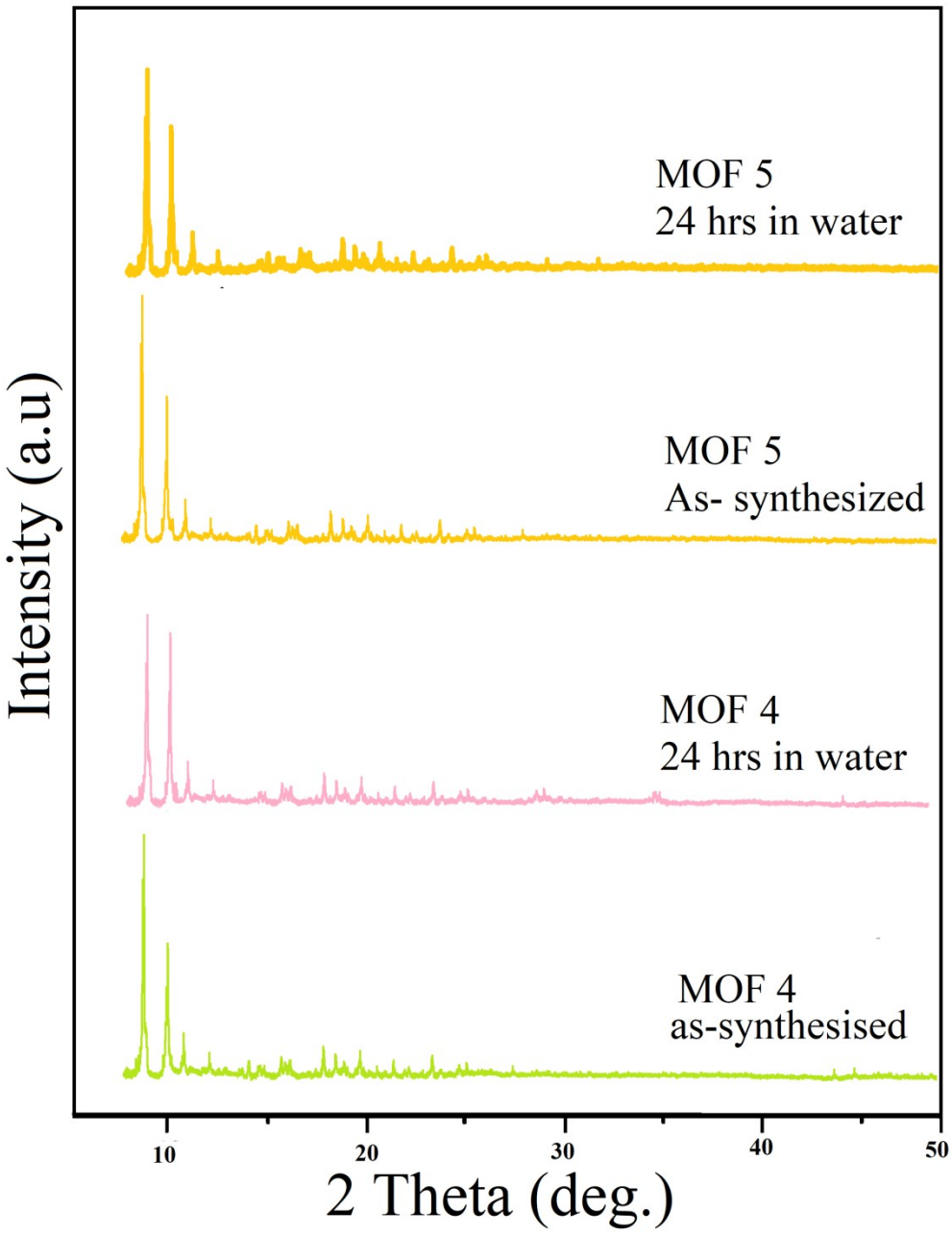

Figure S13. PXRD patterns of MOFs **4** and **5** as-synthesized and in water after 24 h

3. CrystallographicInformation (Tables)

Table S1. Selected Bond lengths (Å) for MOF 1.

O1—Pr1	2.464 (5)	O2W—Pr1	2.477 (5)
O1—Pr1^{i}	2.661 (5)	O4—Pr1^{ii}	2.539 (5)
O2—Pr1^{i}	2.553 (5)	O5—Pr1	2.496 (5)
O1W—Pr1	2.401 (4)	O6—Pr1	2.516 (6)
O3—Pr1^{ii}	2.495 (5)		

Symmetry code(s): (i) $-x+2, -y+1, -z+1$; (ii) $x-1, y, z$.

Table S2. Selected Bond angles (Å) for MOF 1.

O1W—Pr1—O1	84.50 (19)	O3^{iii}—Pr1—O4^{iii}	51.98 (14)
O1W—Pr1—O2W	75.87 (18)	O5—Pr1—O4^{iii}	74.46 (19)
O1—Pr1—O2W	80.3 (2)	O6—Pr1—O4^{iii}	113.85 (18)
O1W—Pr1—O3^{iii}	126.89 (16)	O1W—Pr1—O2^{i}	147.2 (2)
O1—Pr1—O3^{iii}	78.09 (15)	O1—Pr1—O2^{i}	114.75 (15)
O2W—Pr1—O3^{iii}	146.23 (18)	O2W—Pr1—O2^{i}	81.4 (2)
O1W—Pr1—O5	99.5 (2)	O3^{iii}—Pr1—O2^{i}	84.43 (16)
O1—Pr1—O5	152.71 (16)	O5—Pr1—O2^{i}	75.75 (19)
O2W—Pr1—O5	126.9 (2)	O6—Pr1—O2^{i}	73.02 (18)

O3^{iii}—Pr1—O5	78.05 (17)	O4^{iii}—Pr1—O2^{i}	131.07 (17)
O1W—Pr1—O6	78.9 (2)	O1W—Pr1—O1^{i}	138.65 (16)
O1—Pr1—O6	154.23 (15)	O1—Pr1—O1^{i}	65.07 (16)
O2W—Pr1—O6	76.6 (2)	O2W—Pr1—O1^{i}	72.08 (17)
O3^{iii}—Pr1—O6	127.68 (16)	O3^{iii}—Pr1—O1^{i}	75.37 (14)
O5—Pr1—O6	51.12 (16)	O5—Pr1—O1^{i}	120.55 (18)
O1W—Pr1—O4^{iii}	75.94 (16)	O6—Pr1—O1^{i}	117.18 (17)
O1—Pr1—O4^{iii}	80.48 (17)	O4^{iii}—Pr1—O1^{i}	122.04 (16)
O2W—Pr1—O4^{iii}	147.1 (2)	O2^{i}—Pr1—O1^{i}	49.70 (15)

Symmetry code(s): (i) $-x+2, -y+1, -z+1$; (ii) $x-1, y, z$; (iii) $x+1, y, z$.

Table S3. Selected Bond lengths (Å) for MOF 2.

O1—Nd1	2.481 (6)	O4—Nd1	2.503 (7)
O2—Nd1	2.528 (6)	O5—Nd1^{i}	2.453 (6)
O1W—Nd1	2.393 (6)	O5—Nd1^{ii}	2.645 (6)
O3—Nd1	2.481 (7)	O6—Nd1^{ii}	2.538 (6)
O2W—Nd1	2.457 (7)		

Symmetry code(s): (i) $x-1, y, z$; (ii) $-x+1, -y, -z+1$.

Table S4. Selected Bond angles (Å) for MOF 2.

Nd1^{i}—O5—Nd1^{ii}	115.1 (2)	O1—Nd1—O2	52.34 (19)

O1W—Nd1—O5^{iii}	84.4 (2)	O3—Nd1—O2	74.3 (2)
O1W—Nd1—O2W	76.2 (2)	O4—Nd1—O2	114.0 (2)
O5^{iii}—Nd1—O2W	80.1 (3)	O1W—Nd1—O6^{ii}	147.5 (3)
O1W—Nd1—O1	127.1 (2)	O5^{iii}—Nd1—O6^{ii}	114.8 (2)
O5^{iii}—Nd1—O1	78.5 (2)	O2W—Nd1—O6^{ii}	81.4 (3)
O2W—Nd1—O1	145.9 (2)	O1—Nd1—O6^{ii}	83.9 (2)
O1W—Nd1—O3	99.2 (3)	O3—Nd1—O6^{ii}	76.1 (3)
O5^{iii}—Nd1—O3	152.5 (2)	O4—Nd1—O6^{ii}	73.4 (2)
O2W—Nd1—O3	127.3 (3)	O2—Nd1—O6^{ii}	131.1 (2)
O1—Nd1—O3	77.8 (2)	O1W—Nd1—O5^{ii}	138.6 (2)
O1W—Nd1—O4	78.7 (3)	O5^{iii}—Nd1—O5^{ii}	64.9 (2)
O5^{iii}—Nd1—O4	153.8 (2)	O2W—Nd1—O5^{ii}	71.9 (2)
O2W—Nd1—O4	76.5 (3)	O1—Nd1—O5^{ii}	75.06 (19)
O1—Nd1—O4	127.8 (2)	O3—Nd1—O5^{ii}	121.0 (2)
O3—Nd1—O4	51.6 (2)	O4—Nd1—O5^{ii}	117.6 (2)
O1W—Nd1—O2	75.8 (2)	O2—Nd1—O5^{ii}	121.8 (2)
O5^{iii}—Nd1—O2	80.4 (2)	O6^{ii}—Nd1—O5^{ii}	49.87 (19)
O2W—Nd1—O2	147.1 (3)		

Symmetry code(s): (i) $x-1, y, z$; (ii) $-x+1, -y, -z+1$; (iii) $x+1, y, z$.

Table S5. Selected Bond lengths (Å) for MOF 3.

Sm1—O1	2.506 (5)	Sm1—O5	2.466 (6)

Sm1—O2^{i}	2.421 (5)	Sm1—O6	2.486 (6)
Sm1—O2	2.648 (5)	Sm1—O7	2.374 (5)
Sm1—O3	2.452 (5)	Sm1—O8	2.427 (6)
Sm1—O4	2.498 (6)		

Symmetry code(s): (i) −*x*+1, −*y*+1, −*z*+2.

Table S6. Selected Bond angles (Å) for MOF 3.

O2—Sm1—O1	50.02 (16)	O6—Sm1—O4	114.2 (2)
O2^{i}—Sm1—O1	114.87 (17)	O6—Sm1—O5	51.51 (18)
O3—Sm1—O1	84.22 (18)	O7—Sm1—O1	146.6 (2)
O3—Sm1—O2	74.95 (15)	O7—Sm1—O2^{i}	84.9 (2)
O3—Sm1—O2^{i}	78.36 (17)	O7—Sm1—O2	138.74 (18)
O4—Sm1—O1	132.13 (19)	O7—Sm1—O3	127.63 (18)
O4—Sm1—O2	122.22 (17)	O7—Sm1—O4	75.37 (18)
O4—Sm1—O2^{i}	80.14 (19)	O7—Sm1—O5	98.9 (2)
O4—Sm1—O3	53.12 (16)	O7—Sm1—O6	78.3 (2)
O5—Sm1—O1	76.0 (2)	O8—Sm1—O1	81.7 (2)
O5—Sm1—O2^{i}	152.76 (18)	O8—Sm1—O2^{i}	79.3 (2)
O5—Sm1—O2	120.99 (19)	O8—Sm1—O2	71.81 (19)
O5—Sm1—O3	78.09 (18)	O8—Sm1—O3	145.46 (19)
O5—Sm1—O4	74.8 (2)	O8—Sm1—O4	145.7 (2)
O6—Sm1—O1	72.9 (2)	O8—Sm1—O5	127.9 (2)
O6—Sm1—O2^{i}	153.71 (17)	O8—Sm1—O6	77.1 (2)
O6—Sm1—O2	117.29 (19)	O8—Sm1—O7	75.7 (2)

O6—Sm1—O3	127.93 (17)

Symmetry code(s): (i) −*x*+1, −*y*+1, −*z*+2.

Table S**7**. Selected Bond lengths (Å) for MOF **4**.

Eu1—O1W	2.346 (6)	Eu1—O6	2.461 (7)
Eu1—O4	2.402 (6)	Eu1—O1^{i}	2.483 (6)
Eu1—O2W	2.406 (6)	Eu1—O3^{ii}	2.490 (6)
Eu1—O5	2.439 (7)	Eu1—O4^{ii}	2.635 (6)
Eu1—O2^{i}	2.440 (5)		

Symmetry code(s): (i) *x*+1, *y*, *z*; (ii) −*x*+2, −*y*+1, −*z*+1.

Table S**8**. Selected Bond angles (Å) for MOF **4**.

O1W—Eu1—O4	84.8 (2)	O5—Eu1—O1^{i}	74.3 (2)
O1W—Eu1—O2W	76.1 (2)	O2^{i}—Eu1—O1^{i}	53.24 (18)
O4—Eu1—O2W	79.3 (2)	O6—Eu1—O1^{i}	114.3 (2)
O1W—Eu1—O5	98.9 (3)	O1W—Eu1—O3^{ii}	147.1 (2)
O4—Eu1—O5	152.6 (2)	O4—Eu1—O3^{ii}	114.61 (19)
O2W—Eu1—O5	128.0 (2)	O2W—Eu1—O3^{ii}	81.6 (2)
O1W—Eu1—O2^{i}	127.3 (2)	O5—Eu1—O3^{ii}	76.3 (2)
O4—Eu1—O2^{i}	78.46 (19)	O2^{i}—Eu1—O3^{ii}	84.1 (2)

O2W—Eu1—O2^{i}	145.5 (2)	O6—Eu1—O3^{ii}	73.2 (2)
O5—Eu1—O2^{i}	77.8 (2)	O1^{i}—Eu1—O3^{ii}	132.1 (2)
O1W—Eu1—O6	78.2 (3)	O1W—Eu1—O4^{ii}	138.7 (2)
O4—Eu1—O6	152.98 (19)	O4—Eu1—O4^{ii}	64.4 (2)
O2W—Eu1—O6	76.4 (2)	O2W—Eu1—O4^{ii}	71.9 (2)
O5—Eu1—O6	52.4 (2)	O5—Eu1—O4^{ii}	121.3 (2)
O2^{i}—Eu1—O6	128.6 (2)	O2^{i}—Eu1—O4^{ii}	74.87 (18)
O1W—Eu1—O1^{i}	74.9 (2)	O6—Eu1—O4^{ii}	117.6 (2)
O4—Eu1—O1^{i}	80.6 (2)	O1^{i}—Eu1—O4^{ii}	122.23 (19)
O2W—Eu1—O1^{i}	145.9 (2)	O3^{ii}—Eu1—O4^{ii}	50.24 (18)

Symmetry code(s): (i) x+1, y, z; (ii) −x+2, −y+1, −z+1.

Table S**9**. Selected Bond lengths (Å) for MOF **5**.

O1—Tb1	2.415 (9)	O4—Tb1	2.413 (7)
O2—Tb1	2.449 (9)	O5—Tb1^{i}	2.458 (8)
O1W—Tb1	2.329 (8)	O6—Tb1	2.366 (8)
O3—Tb1	2.457 (8)	O6—Tb1^{ii}	2.628 (8)
O2W—Tb1	2.378 (9)		

Symmetry code(s): (i) −x+2, −y, −z+2; (ii) −x+1, −y, −z+2.

Table S**10**. Selected Bond angles (Å) for MOF **5**.

Tb1—O6—Tb1^{ii}	116.4 (3)	O4—Tb1—O3	53.8 (3)
O1W—Tb1—O6	85.3 (3)	O1—Tb1—O3	74.2 (3)
O1W—Tb1—O2W	75.8 (3)	O2—Tb1—O3	114.6 (3)
O6—Tb1—O2W	78.4 (3)	O1W—Tb1—O5^{i}	146.6 (3)
O1W—Tb1—O4	127.8 (3)	O6—Tb1—O5^{i}	114.3 (3)
O6—Tb1—O4	78.7 (3)	O2W—Tb1—O5^{i}	81.7 (3)
O2W—Tb1—O4	145.1 (3)	O4—Tb1—O5^{i}	84.0 (3)
O1W—Tb1—O1	98.7 (4)	O1—Tb1—O5^{i}	76.5 (3)
O6—Tb1—O1	152.6 (3)	O2—Tb1—O5^{i}	73.1 (3)
O2W—Tb1—O1	128.9 (3)	O3—Tb1—O5^{i}	132.6 (3)
O4—Tb1—O1	77.5 (3)	O1W—Tb1—O6^{ii}	138.7 (3)
O1W—Tb1—O2	77.7 (4)	O6—Tb1—O6^{ii}	63.6 (3)
O6—Tb1—O2	152.5 (3)	O2W—Tb1—O6^{ii}	71.9 (3)
O2W—Tb1—O2	76.5 (3)	O4—Tb1—O6^{ii}	74.5 (3)
O4—Tb1—O2	128.8 (3)	O1—Tb1—O6^{ii}	121.5 (3)
O1—Tb1—O2	53.1 (3)	O2—Tb1—O6^{ii}	117.8 (3)
O1W—Tb1—O3	74.8 (3)	O3—Tb1—O6^{ii}	122.1 (3)
O6—Tb1—O3	80.9 (3)	O5^{i}—Tb1—O6^{ii}	50.6 (3)
O2W—Tb1—O3	145.2 (3)		

Symmetry code(s): (i) −*x*+2, −*y*, −*z*+2; (ii) −*x*+1, −*y*, −*z*+2.

Table S11. Hydrogen bonding parameters of MOF **1**

D—H···*A*	*D*—H (Å)	H···*A* (Å)	*D*···*A* (Å)	*D*—H···*A* (°)
O1W--H1WA..O5 [i]	0.82	1.89	2.6898(1)	172
O1W--H1WB..N1 [iv]	0.82	1.88	2.9236(1)	167
O2W--H2WA..O3 [ii]	0.81	2.20	2.9236(1)	148
O2W--H2WB..O1 [iii]	0.81	2.39	2.9593(1)	128
O2W--H2WB..O1 [iii]	0.81	2.41	3.0257(1)	133

Symmetry code(s): (i) 1+x,y,z ; (ii) 1-x,-y,1-z; (iii) -x,-y,1-z; (iv) 1-x,-y,2-z.

Table S12. Hydrogen bonding parameters of MOF **2**

D—H···*A*	*D*—H (Å)	H···*A* (Å)	*D*···*A* (Å)	*D*—H···*A* (°)
O1W --H1W ..N1[iii]	0.82	1.88	2.6931(1)	169
O1W --H1WB..O3[i]	0.82	1.89	2.7047(1)	175
O2W --H2WA..O1[ii]	0.82	2.17	2.9462(1)	158
O2W--H2WA..O6[ii]	0.82	2.45	2.9343(1)	118

Symmetry code(s): (i) -1+x,y,z ;(ii) -x,-y,1-z; (iii) -x,-y,-z.

Table S13. Hydrogen bonding parameters of MOF **3**

D—H···*A*	*D*—H (Å)	H···*A* (Å)	*D*···*A* (Å)	*D*—H···*A* (°)
O(7)--H(7A)..O(5)[i]	0.85	1.90	2.7158(1)	161
O(7 --H(7B)..N(1)[ii]	0.85	2.16	2.6980(1)	121
O(8) --H(8B)..O(2)[ii]	0.85	2.60	2.9613(1)	107
O(8) --H(8B)..O(3)[i]	0.85	2.10	2.9080(1)	160

Symmetry code(s): (i) 1+x,y,z; (ii) 1+x,y,1+z.

Table S14. Hydrogen bonding parameters of MOF **4**

D—H···*A*	*D*—H (Å)	H···*A* (Å)	*D*···*A* (Å)	*D*—H···*A* (°)
O1W--H1WA ..N1 ^{iv}	0.82	1.90	2.6904(1)	162
O1W--H1WB..O5 ^{i}	0.82	1.91	2.7992(1)	173
O2W--H2WA ..O2^{iii}	0.81	2.31	2.9069(1)	131
O2W --H2WB ..O3 ^{ii}	0.81	2.26	2.9635(1)	144
O2W--H2WB..O3 ^{iii}	0.82	2.26	2.9498	143

Symmetry code(s): (i) 1+x,y,z; (ii) 1-x,-y,1-z; (iii) 2-x,-y,1-z; (iv) 2-x,-y,2-z.

Table S15. Hydrogen bonding parameters of MOF **5**

D—H···*A*	*D*—H (Å)	H···*A* (Å)	*D*···*A* (Å)	*D*—H···*A* (°)
O1W--H1WA ..O1^{ii}	0.82	1.91	2.7189(1)	171
O1W--H1WB..N1^{iii}	0.82	1.87	2.6818(1)	172
O2W--H2WA..O6^{i}	0.82	2.32	2.9461(1)	133
O2W --H2WB..O5^{ii}	0.81	2.31	2.9566(1)	137
O2W--H2WB..O4 ^{i}	0.81	2.23	2.8844(1)	137

Symmetry code(s): (i) 1-x,-y,2-z; (ii) -1+x,y,z; (iii) 1-x,-y,1-z .

4. Previous MOF-based sensors for Pb^{2+} detection Table

Table S16 Comparison of Quenching Efficiencieswith previously reported literature.

MOF	**Stern -Volmer Constant (Ksv)L/mol**	**Analyte**	**Ref.**
$[Eu_2(FDC)_3DMA(H_2O)_3]\cdot DMA\cdot 4.5H_2O$	2.97×10^3	Pb^{2+}	**4**
$[Cd_3(5\text{-}NH_2\text{-}mdc)_3(Bipy)_3\cdot H_2O]n$	9.970×10^3	Pb^{2+}	**5**
$\{[(CH_3)2NH_2]_3(In_3L_4)\}\cdot$(solvent)x	9.78×10^3	Pb^{2+}	**6**
NH_2-MIL-53(Cr)	7.48×10^3	Pb^{2+}	**7**

$[Zn(HL_2)(bipy)0.5(H_2O)]\cdot 2H_2O$	1.18×10^4	Pb^{2+}	**8**
This work	8.90×10^3	Pb^{2+}	This work
This work	5.47×10^4	Pb^{2+}	This work

5.Stern -Volmer Constants, Quenching Efficiencies and LODs Table

Table S17 Stern -Volmer Constants, Quenching Efficiencies and LODs Tables

CP-4 with Heavy metal analyte	**Stern -Volmer Constant (K_{sv}) L/mol**	**Quenching Efficiency (%)**	**LOD(ppm)**
Pb^{2+}	8.90×10^3	74.5%	0.014
Cd^{2+}	2.79×10^3	54.00%	0.069
Hg^{2+}	1.92×10^3	54.35%	0.20
Mn^{2+}	8.91×10^2	53.95%	1.03
Ni^{2+}	2.38×10^2	53.24%	1.15

CP-5 with Heavy metal analyte	**Stern -Volmer Constant (K_{sv}) L/mol**	**Quenching Efficiency (%)**	**LOD(ppm)**
Pb^{2+}	5.47×10^4	95.1%	0.013
Hg^{2+}	1.62×10^4	86.39%	0.098
Ni^{2+}	3.65×10^2	63.49%	1.23
Cd^{2+}	3.12×10^3	57.49%	1.29
Mn^{2+}	1.31×10^3	52.37%	2.12

References:

1. C. Li, T. Chen, W. Xu, X. Lou, L. Pan, Q. Chen and B. Hu, *J. Mater. Chem. A*, 2015, **3**, 5585–5591.
2. L. Peng, J. Zhang, Z. Xue, B. Han, J. Li and G. Yang, *Chem.Commun*., 2013, **49**, 11695.
3. V. I. Isaeva, E. V. Belyaeva, A. N. Fitch, V. V. Chernyshev, S. N. Klyamkin, and L. M. Kustov, *Cryst. Growth Des.* 2013, **13**, 5305–5315.
4. L. Li, Q. Chen, Z. Niu, X. Zhou, T. Yang and W. Huang, *J. Mater. Chem. C*, 2016, **4**, 1900-1905.
5. K.A.Nartey, X.Wang, J. Zhang and J. Hu, *Opt. Mater.,*2021, **119**, 111327.
6. Q. Li, B. Guan, W. Zhu, T. Liu, L. Chen, Y. Wang and D. Xue, *J. Solid State Chem.*, 2020,**291**, 121672.

7. H. Guo, D. Wang, J. Chen, W. Weng, M. Huang and Z. Zheng, *Chem. Eng. J.,*2016, **289** 479-485.
8. J.X. Hou, J.P. Gao, J. Liu, X. Jing, L. J. Li and J.L. Du, *Dyes Pigm*., 2019, **160**, 159-164.